CHAPTER 8

PHOTOSYNTHESIS AND CARBON BALANCE

J. MÜLLER, P. WERNECKE, H. BRAUNE AND W. DIEPENBROCK

Institute of Agronomy and Crop Science
Martin-Luther-University of Halle-Wittenberg, Germany

Abstract. The requirements for modelling photosynthesis and related processes within the framework of a Functional-Structural Plant Model (FSPM; cf. Vos et al. this volume) are discussed. A combined local **g**as (carbon dioxide, water vapour) and **r**adiant energy **e**xchange **m**odel (GREM) is presented, that was specified to be embedded into an FSPM. The model accounts for the effect of organ nitrogen content (*N*) on gas exchange expressing certain key model parameters as functions of *N*. This approach enables the model also to account for the observed effects of growth conditions and organ development on gas exchange, since such effects could to a large part be ascribed to concurrent changes in *N*. The GREM was parameterized for leaf blades of barley (*Hordeum vulgare* L.) plants. The combined FSPM-GREM system was successfully applied in simulation studies providing reliable predictions of (1) diurnal time courses of carbon dioxide and water vapour exchange of leaf blades and (2) overall carbon balance and dry-mass accumulation of barley plants during ontogenesis.

INTRODUCTION

FSPMs describe the functional and structural organization of biological systems as a dynamic three-dimensional framework of interacting units (e.g. organs). This way, FSPMs offer a novel access to the simulation of plant development, growth and exchange of radiant energy, carbon dioxide, water vapour, and other physical entities between plants and the environment. However, the potential of FSPMs in modelling the spatial and temporal patterns of plants will not be utilized adequately calculating photosynthesis by simple relations, as, for example, the light-use-efficiency approach. Instead, the photosynthesis model should reflect the inherent non-linear and interrelated responses to environmental factors. Thus, for modelling photosynthesis at organ (e.g. leaf) level, the processes of gas (photosynthesis, respiration, transpiration) and radiative-energy exchange must be described by the combined GREM approach. This can be achieved by coupling the biochemical leaf photosynthesis model of Farquhar et al. (1980; in short: FCB model), the stomatal model of Jarvis (1976) or Ball et al. (1987; in short: BWB model), and an energy

J. Vos, L.F.M. Marcelis, P.H.B. de Visser, P.C. Struik and J.B. Evers (eds.), Functional-Structural Plant Modelling in Crop Production, 91-101.

and mass transport sub-model. Combined models of this type were proposed by Collatz et al. (1991) and Nikolov et al. (1995).

In the current paper, the specific requirements to a GREM for coupling with the FSPM approach are discussed and an example of a coupled FSPM-GREM system is given. The system was specified for spring barley (*Hordeum vulgare* L., cv. 'Barke'). Simulation results on local photosynthetic carbon gain and carbon balance of plants obtained by means of a combined FSPM-GREM system are presented.

MODEL DESCRIPTION

Requirements to the formulation of the GREM

FSPMs treat plants as a collection of organ-related individual units interacting with each other and with the local environment. With respect to the physical environment perceived by each aerial organ of a plant population, Chelle (2005) introduced the terms phylloclimate and phylloclimate model (PCM). Several projects initiated during the last years deal with coupling FSPM and PCM (cf. Chelle 2005 for review). Though this promising development is yet in progress, it should facilitate to relate the organ-scale biophysical and biochemical processes considered by the above-defined GREM component of the FSPM to the local phylloclimate variables affecting organ functions. Thus, required features of a GREM are: i) physical input variables corresponding to local phylloclimate variables that act on gas and energy exchange; ii) physical state variables and biological characteristics that control the functionality of the 'physiological machinery' at organ scale (the biological characteristics are additional inputs to the GREM); and iii) outputs in terms of gas and radiative-energy fluxes. The system to be described by a GREM is presented schematically in Figure 1 (radiative-energy fluxes, gas fluxes and biological state variables printed in bold).

While the physical input variables may be easily specified, the choice of appropriate characteristics defining the biological system is less clear and, to some extent, depends on the considered detail at organ scale. In particular, these characteristics must account for effects of organ development, mineral nutrition and adaptation to growth conditions on gas and radiative-energy exchange. A way to account for these diverse relationships may be to relate the manifold responses of the biological system to certain basic physiological state variables controlling the observed patterns. In a first step, we may choose such characteristics like chlorophyll and nitrogen content, specific organ (leaf) area, stomatal conductance and others. However, further refinement may be required, in particular if the three-dimensional structure of plant organs is considered (e.g. Juurola et al. 2005). Selecting nitrogen content as a key state variable assumed to be closely related to the potential activity of physiological processes, we follow a common practice in crop growth modelling (review: Jeuffroy et al. 2002). Indeed, many studies reveal that the variation of net photosynthesis with species, seasons and growth conditions is related to concurrent changes in leaf nitrogen content (e.g. Niinemets and Tenhunen 1997; Medlyn et al. 1999; Meir et al. 2002). On this basis, it was hypothesized (Müller et al. 2005), that the variation of potential leaf photosynthesis along with

changing environment or growth conditions, but also with respect to leaf rank and leaf senescence, might to a large part be related to underlying effects of leaf nitrogen dynamics on photosynthesis. If so, it should be possible to account for these relationships by introducing nitrogen sensitivity into the GREM. A specification of this approach will be given in the next section.

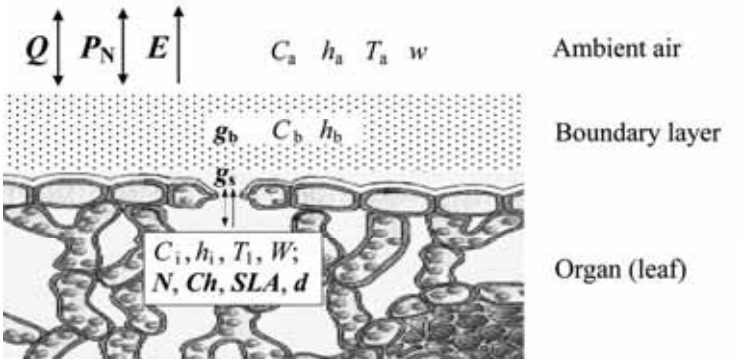

Figure 1. *Photosynthetic apparatus of a leaf, gas and radiative-energy fluxes, input variables and state variables related to the GREM. Q is total radiation flux (photosynthetically active (Q_p), near infrared and thermal infrared), P_N and E are net photosynthesis and transpiration rate, respectively, C_a, C_b, C_i, and h_a, h_b, h_i are CO_2 content and relative humidity of ambient air (subscript a), of air within leaf boundary layer (subscript b), or of the air within leaf intercellular spaces (subscript i), respectively. T_a and T_l are the temperature of the ambient air and of the leaf, g_s and g_b are stomatal and boundary-layer conductance, and w is the wind speed of ambient air. W is leaf water potential, and N and Ch are leaf nitrogen and chlorophyll concentration per unit leaf area, respectively. SLA is specific leaf area (area per unit mass) and d is leaf width. The ellipsoid structures are the chloroplasts representing distributed sites of photochemical conversion of light energy and biochemical CO_2 fixation within mesophyll cells. The transport of CO_2 between intercellular spaces and reaction sites in the liquid phase of mesophyll cells is not considered in the scheme*

Specification of the GREM

Most of above-discussed demands to a GREM are met by the LEAFC3 model of Nikolov et al. (1995). This model combines all major processes and interactions related to leaf CO_2, water vapour and radiative-energy exchange on the basis of a coupled FCB-BWB model, including also a detailed sub-model of boundary-layer gas and radiative-energy transfer. The model assumes steady-state conditions, such that the net rates of biochemical CO_2 fixation and CO_2 transport between external air and reaction sites may be assumed equal. For simplification, the model approximates CO_2 concentration at the sites of carboxylation within the chloroplasts by that of intercellular spaces. The LEAFC3 model was extended by developing the nitrogen-sensitive version LEAFC3-N (Müller et al. 2005).

Linking the above-mentioned processes leads to a complex system of coupled non-linear equations, which must be solved simultaneously. A general formulation

of this equation system is listed below (symbols as in Figure 1, unknown variables printed in bold):

$$\boldsymbol{P_N} = f(Q_{P,a}, C_a, \boldsymbol{C_i}, \boldsymbol{T_l}; N) \quad (1)$$

$$\boldsymbol{E} = f(h_a, T_a, \boldsymbol{T_l}, \boldsymbol{g_s}, \boldsymbol{g_b}) \quad (2)$$

$$\boldsymbol{C_i} = f(C_a, \boldsymbol{P_N}, \boldsymbol{g_s}, \boldsymbol{g_b}) \quad (3)$$

$$\boldsymbol{g_s} = f(W, \boldsymbol{P_N}, \boldsymbol{h_b}, \boldsymbol{C_b}; N) \quad (4)$$

$$\boldsymbol{h_b} = f(\boldsymbol{E}, h_a, \boldsymbol{g_s}, \boldsymbol{g_b}, \boldsymbol{T_l}) \quad (5)$$

$$\boldsymbol{C_b} = f(C_a, \boldsymbol{P_N}, \boldsymbol{g_b}) \quad (6)$$

$$\boldsymbol{T_l} = f(Q, T_a, \boldsymbol{E}, \boldsymbol{g_s}, \boldsymbol{g_b}) \quad (7)$$

$$\boldsymbol{g_b} = f(w, T_a, \boldsymbol{T_l}; d) \quad (8)$$

Equation 1 is defined by the FCB model, where absorbed photon flux $Q_{P,a}$ is calculated from Q_P and leaf absorptance given as a function of *Ch*. *Ch* and *N* are defined on one-sided leaf area basis and equivalent to the corresponding dry-mass-related characteristics divided by *SLA*. To calculate P_N, the FCB model uses mitochondrial respiration rate R_{d25} of the photosynthetic organ (omitted in Equation 1). Equation 2 calculates *E* from vapour pressure gradient between intercellular spaces and external air, Equations 3 and 6 calculate C_i or C_b, respectively, equating net CO_2 transport and fixation rates, Equation 4 is the BWB model, Equation 5 provides h_b, Equation 7 solves for leaf energy balance, and Equation 8 calculates g_b accounting for both forced and free convective exchanges. Introducing a simple method to the exact solution of the leaf energy balance equation and several other simplifications, the number of time-intensive nested iterations was reduced, thus obtaining an efficient solution algorithm of the model (cf. Nikolov et al. 1995; Müller et al. 2005).

Effects of *N* were included into the model replacing certain key parameters by nitrogen-dependent functions. These functions were derived from comprehensive measurements of the response of P_N and *E* to Q_P and C_i. Measurements were done on leaf blades of the main tiller of barley plants during the entire course of leaf development and plant ontogenesis. Experimental and parameterization procedures mainly followed those described by Müller et al. (2005).

Specifying the model parameterization for barley leaves, the variation of maximum carboxylation rate V_{m25} (subscript 25: reference temperature 25 °C) along with both leaf rank and leaf senescence could be attributed to concomitant changes in *N* (Figure 2a). This correlation has a clear theoretical basis, since it is a well-known fact that most nitrogen in leaves is bound by Rubisco. The slope of the empirical relationship given in Figure 2a agrees well with theoretical estimates (cf.

Müller et al. 2005). However, our recent analyses indicate that this relationship may be less strong during a period of one or two weeks after leaf emergence. The correlation between V_{m25} and N indirectly describes also the concurrent variation in maximum electron transport rate J_{m25} commonly related to V_{m25} by a factor of about two (Leuning 1997). Here, this factor was found to remain unchanged for a range of nitrogen nutrition (50 - 200 mg plant^{-1}) and to vary from 2.8 to 1.9 for different growth temperatures (13 - 22 °C). Maximum quantum yield of photosynthetic electron transport φ_a (mol electrons (mol absorbed quanta)$^{-1}$) also revealed a close relation to V_{m25} (Figure 2b). Therefore, this characteristic was included into the model instead of the observed weaker correlation between φ_a and N. The relationships between V_{m25} and J_{m25} or φ_a, respectively, may be attributed to a coordinated degradation of photosynthetic apparatus during leaf senescence. Following the formulation in LEAFC3, R_{d25} was related to V_{m25} as well, where the ratio of R_{d25} to V_{m25} also depends on N. Finally, a unique nitrogen-dependent parameterization of the BWB stomatal-conductance model (cf. Müller et al. 2005) was obtained (results not shown).

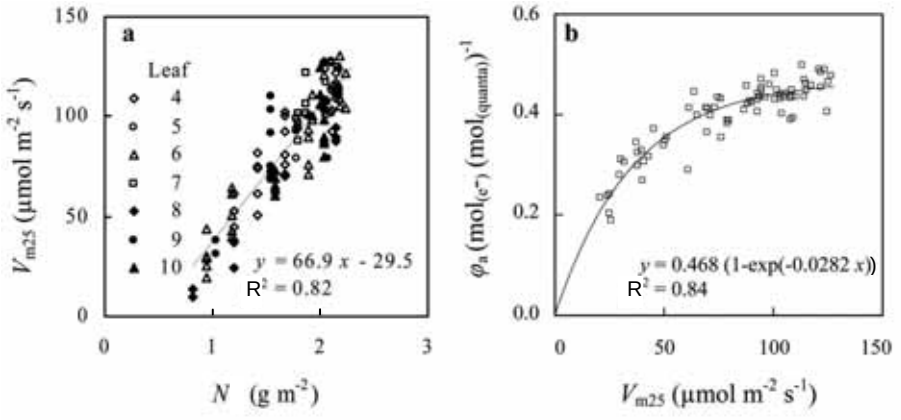

Figure 2. *Two key relationships of the nitrogen-sensitive parameterization of the photosynthesis model: a) maximum carboxylation rate V_{m25} vs. nitrogen concentration per unit leaf area, N; b) maximum quantum yield of electron transport φ_a vs. V_{m25}*

COUPLING WITH AN FSPM

For simulation studies discussed in the present paper, the barley LEAFC3-N model was coupled to the FSPM system VICA (Figure 3; cf. also Wernecke this volume). To evaluate the model specifically with respect to its accuracy in predicting carbon assimilation, we used a simplified FSMP-GREM model configuration, thus avoiding uncertainties related to other components of the FSPM. Inputs to the GREM were: i) T_a, C_a, h_a and w (hourly means of measurements, w assumed constant), ii) $Q_{P,a}$ for each polygon (calculated by VICA, hourly means), iii) polygon area (calculated by

VICA, daily values), and iv) leaf *N*. Focusing here mainly on carbon economy, instead of simulated *N* we used measurements interpolated to daily values. Further, for the special conditions of the glasshouse experiment, the calculation of radiative-energy balance was omitted, approximating T_l by T_a.

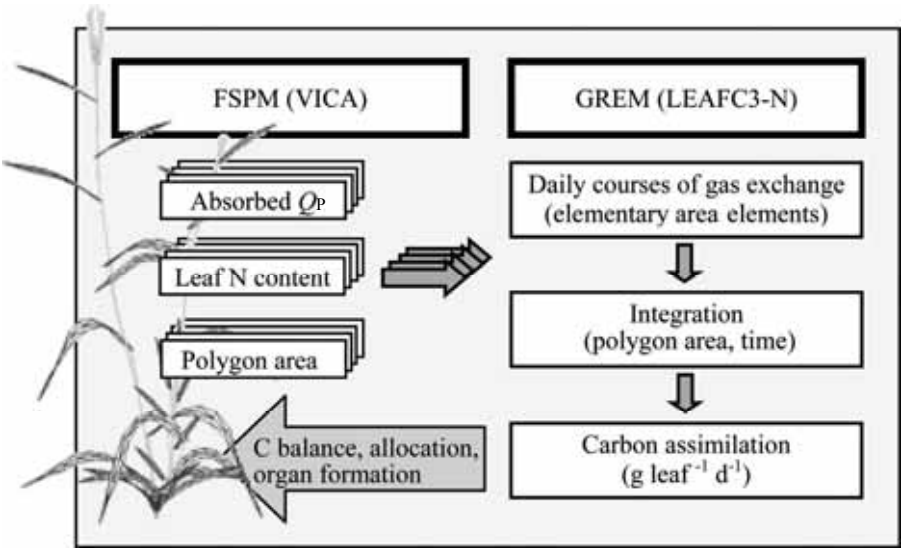

Figure 3. *FSPM-GREM coupling scheme*

SIMULATION RESULTS

Gas exchange

Based on the combined FSPM-GREM system specified above, diurnal time courses of net photosynthesis rate P_N (Figure 4) and transpiration rate E (results not shown) of all leaves were simulated for uniculm barley plants grown in a glasshouse experiment (for experimental detail, see Wernecke et al. this volume). Maximum rates of P_N in order of 20 μmol m^{-2} s^{-1} correspond well with the values observed under comparable conditions. The sequential activity pattern of P_N of the individual leaf blades and the effect of leaf senescence may be clearly recognized from Figure 4.

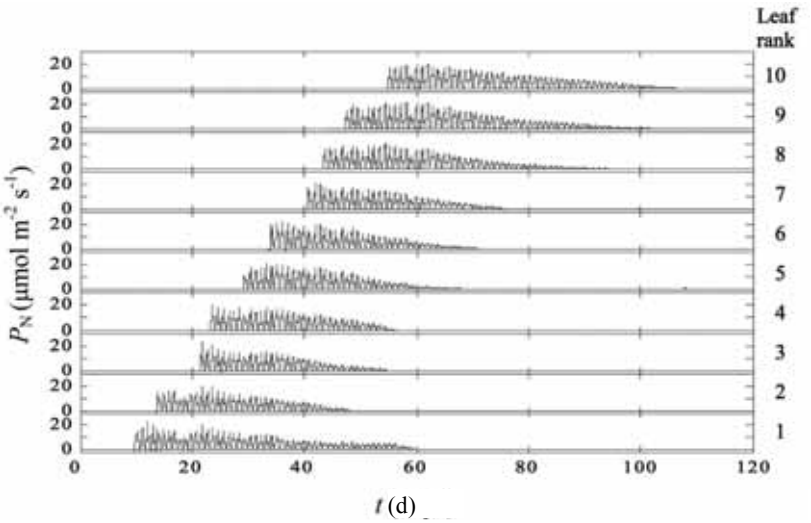

Figure 4. *Simulated diurnal time courses (hourly means) of net photosynthesis rate P_N of leaf blades, leaf rank 1 to 10. Time t: days after sowing*

Carbon balance and dry-mass accumulation

To assess model performance in estimating carbon gain, we simulated total plant carbon and dry-mass accumulation during entire ontogenesis. Plant gross photosynthesis rate A_g (carboxylation rate minus photorespiration rate) was obtained by summing up A_g of individual organs. A_g of leaf blades and sheaths was calculated by LEAFC3-N. A_g of the ear was assumed to be in order of that of the leaf blade of the flag leaf. Carbon losses due to mitochondrial respiration were estimated according to the concept of growth and maintenance respiration (R_g, R_m), providing a simple yet robust approach (review: Cannell and Thornley 2000; Yin and Van Laar 2005). Note that R_g and R_m in contrast to R_{d25} refer to the whole plant. With regard to common ranges given in literature, R_g was assumed to consume about 25 % of total carbon assimilated per day. The contribution of different physiological processes to R_m up to now is difficult to quantify. Therefore, only a lumped R_m term was considered, where the resulting carbon loss was assumed proportional to nitrogen mass of individual organs (leaves, ear, pseudostem, root). The corresponding proportionality coefficient k_{Rm} cannot be specified mechanistically from available data. Therefore, its value was estimated based on the range of k_{Rm} = 0.2 - 0.6 g C (g N)$^{-1}$ d^{-1} given in literature (cf. Cannel and Thornley 2000), applying some empirical adjustment. The effect of senescence on R_m was included by a scaling function of the form $f_{Rm} = (N_m - N_{m,min})/(N_{m,max} - N_{m,min})$, $0 \le f_{Rm} \le 1$, where N_m is organ nitrogen content on dry-mass basis. $N_{m,max}$ and $N_{m,min}$ are coefficients representing the observed maximum and minimum values of N_m, respectively. Because of the above-mentioned uncertainty of k_{Rm}, simulations of carbon accumulation are given for a range of k_{Rm} values (Figure 5a). Plant dry mass was

approximated from simulated carbon mass based on observed organ-scale carbon content. Figure 5b gives the results obtained from best model-estimated carbon gain (k_{Rm} = 0.5 g C (g N)$^{-1}$ d^{-1}). The simulation results confirm the functionality of the combined FSPM-GREM system in assessing plant carbon gain as well as the used range of parameter values.

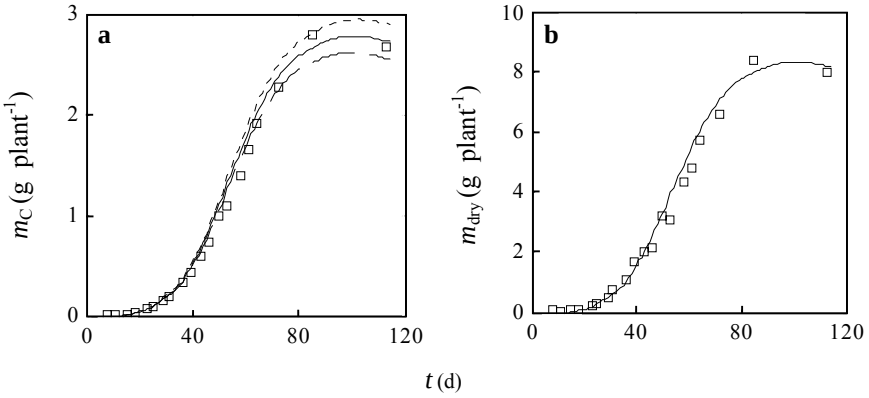

Figure 5. *Measurements (squared symbols, means of four replicates each comprising four or five plants) and simulations (lines) of (a) carbon mass m_C (k_{Rm} = 0.45 (dotted), 0.5 (solid) and 0.55 (dashed) g C (g N)$^{-1}$ d^{-1}) and (b) dry mass m_{dry} per plant. Time t: days after sowing*

DISCUSSION

The key parameters of the LEAFC3-N model derived for barley leaves are within the range of those obtained previously for leaves of wheat (Müller et al. 2005) and oilseed rape (Müller and Diepenbrock 2006). The values of the slope of the V_{m25} vs N relationship and of the maximum quantum yield φ_a correspond closely with those expected theoretically (cf. Müller et al. 2005). However, within this context we must return to the point that the present model approximates the CO_2 concentration at the sites of carboxylation within the chloroplasts by that of the air within the intercellular spaces. As recently demonstrated by Juuorola et al. (2005), biochemical parameters and their temperature dependencies estimated this way implicitly include both effects of CO_2 dissolution at the air–cell-surface interface and of transport within mesophyll cells. The latter is limited by the mesophyll liquid-phase diffusive conductance g_i. However, g_i is rarely known (Bunce 2000; Bernacchi et al. 2003), and thus LEAFC3-N retains the approach of neglecting the limitation by g_i as most other contemporary eco-physiological gas exchange models do. Therefore, the Rubisco-related parameters derived from gas exchange measurements in fact represent apparent leaf characteristics differing to some extent from those determined exclusively by biochemical characteristics (cf. Von Caemmerer 2000, Table 1.3; Juurola et al. 2005). Though this restricts a purely mechanistic interpretation of obtained parameter estimates, it will not affect the performance of

the model in predicting reliably the eco-physiological patterns of gas and energy exchange.

Based on the current study, the LEAFC3-N model was proved to operate successfully as part of an FSPM and to provide reliable predictions of both net photosynthesis rate P_N and transpiration rate E (results for E not shown). Focussing here mainly on the accuracy of model-predicted carbon balance, a robust approach was applied to describe plant architecture based on measured geometrical characteristics. In contrast, the complete version of VICA is capable of accounting for the feedback of carbon-driven organ formation (cf. Wernecke et al. this volume).

Future improvements in simulating carbon assimilation will focus mainly on the following subjects. At first, the calculation of photosynthetic contribution of leaf sheaths and ears clearly should be refined. While the geometrical characteristics of these organs are provided quite precisely by the architectural component of the FSPM, most uncertainty arises from a lack of information about physiological characteristics of these organs. This may be not as critical for leaf sheaths as for ears, because it probably will be justified to treat the photosynthetic apparatus of leaf sheaths similar to that of leaf blades. Nevertheless, this assumption should be confirmed. Further, it is clear that structural and functional properties of the individual components of the ear, in particular of the awns, should be addressed appropriately, provided reliable experimental information becomes available.

A second point serving special attention is the precise determination of respiration coefficients, to which simulated carbon accumulation is highly sensitive. Since from our data growth and maintenance respiration coefficients could not be estimated independently of each other, used values were adopted from literature. In principle, these coefficients may be calculated on a mechanistic basis from underlying biochemistry and physiology, but many aspects up to now remain uncertain (cf. Yin and Van Laar 2005). Thus, following Yin and Van Laar (2005), a practicable trade-off may be using average, but different growth respiration coefficients for vegetative organs and seeds based on chemical composition of plant material. Several maintenance respiration components in principle may be derived from underlying physiology as well, but some others are difficult to specify. Further, effects of organ or plant development on respiration components should be accounted for by more mechanistic approaches than are used here.

To refine the treatment of respiration this way will require introducing more biochemical and physiological detail into the FSPM. Thus, extension of the GREM towards a generic organ-scale network model of combined carbon and nitrogen metabolism will be a logic consequence for future development. However, though FSMPs generally provide an excellent platform for including physiological detail at different scales, such refinement should be treated with caution. With limited observations and unsatisfactory information for reliable parameterization, degrees of freedom in parameter specification will increase, such that it may be impossible to identify a unique parameter set (Mo and Beven 2004). In that case, many different parameter sets, from physiologically feasible ranges, may provide an acceptable behaviour of the model, but the robustness and analytical power of the modelling approach will diminish.

Several developments of the FSPM in progress can only be realized based on the integrated FSPM-GREM system (cf. also Wernecke et al. this volume). With regard to the complementary development of the GREM, this concerns the interrelation between carbon assimilation and organ formation, the control of organ-related gas exchange processes by plant nitrogen economy, the interface between phylloclimate, local geometrical surface characteristics and leaf boundary layer mechanisms, and finally the solution of the combined water and energy balance at organ, plant and canopy scale.

ACKNOWLEDGEMENTS

The authors thank Dr. K. Egle and Dr. H. Beschow, Institute of Soil Science and Plant Nutrition, Martin-Luther-University of Halle-Wittenberg, for analyses of carbon and nitrogen content. The study was funded by the German Research Association (Deutsche Forschungsgemeinschaft, DFG 472 DI 294/22) and the state of Saxony-Anhalt.

REFERENCES

Ball, J.T., Woodrow, I.E. and Berry, J.A., 1987. A model predicting stomatal conductance and its contribution to the control of photosynthesis under different environmental conditions. *In:* Biggins, J. ed. *Progress in photosynthesis research: proceedings of the 7th International congress on photosynthesis providence, Rhode Island, USA, August 10 - 15, 1986*. Nijhoff, Dordrecht, 221-224.

Bernacchi, C.J., Pimentel, C. and Long, S.P., 2003. *In vivo* temperature response functions of parameters required to model RuBP-limited photosynthesis. *Plant, Cell and Environment,* 26 (9), 1419-1430.

Bunce, J.A., 2000. Acclimation of photosynthesis to temperature in eight cool and warm climate herbaceous C3 species: temperature dependence of parameters of a biochemical photosynthesis model. *Photosynthesis Research,* 63 (1), 59-67.

Cannell, M.G.R. and Thornley, J.H.M., 2000. Modelling the components of plant respiration: some guiding principles. *Annals of Botany,* 85 (1), 45-54.

Chelle, M., 2005. Phylloclimate or the climate perceived by individual plant organs: what is it? how to model it? what for? *New Phytologist,* 166 (3), 781-790.

Collatz, G.J., Ball, J.T., Grivet, C., et al., 1991. Physiological and environmental regulation of stomatal conductance, photosynthesis and transpiration: a model that includes a laminar boundary layer. *Agricultural and Forest Meteorology,* 54 (2/4), 107-136.

Farquhar, G.D., Von Caemmerer, S. and Berry, J.A., 1980. A biochemical model of photosynthetic CO_2 assimilation in leaves of C3 species. *Planta,* 149 (1), 78-90.

Jarvis, P.G., 1976. The interpretation of the variations in leaf water potential and stomatal conductance found in canopies in the field. *Philosophical Transactions of The Royal Society of London, B,* 273 (927), 593-610.

Jeuffroy, M.H., Ney, B. and Ourry, A., 2002. Integrated physiological and agronomic modelling of N capture and use within the plant. *Journal of Experimental Botany,* 53 (370), 809-823.

Juurola, E., Aalto, T., Thum, T., et al., 2005. Temperature dependence of leaf-level CO_2 fixation: revising biochemical coefficients through analysis of leaf three-dimensional structure. *New Phytologist,* 166 (1), 205-215.

Leuning, R., 1997. Scaling to a common temperature improves the correlation between the photosynthesis parameters J_{max} and V_{cmax}. *Journal of Experimental Botany,* 48 (307), 345-347.

Medlyn, B.E., Badeck, F.W., De Pury, D.G.G., et al., 1999. Effects of elevated CO_2 on photosynthesis in European forest species: a meta-analysis of model parameters. *Plant, Cell and Environment,* 22 (12), 1475-1495.

Meir, P., Kruijt, B., Broadmeadow, M., et al., 2002. Acclimation of photosynthetic capacity to irradiance in tree canopies in relation to leaf nitrogen concentration and leaf mass per unit area. *Plant, Cell and Environment,* 25 (3), 343-357.

Mo, X. and Beven, K., 2004. Multi-objective parameter conditioning of a three-source wheat canopy model. *Agricultural and Forest Meteorology,* 122 (1/2), 39-63.

Müller, J. and Diepenbrock, W., 2006. Measurement and modelling of gas exchange of leaves and pods of oilseed rape. *Agricultural and Forest Meteorology,* 139 (3/4), 307-322.

Müller, J., Wernecke, P. and Diepenbrock, W., 2005. LEAFC3-N: a nitrogen-sensitive extension of the CO_2 and H_2O gas exchange model LEAFC3 parameterised and tested for winter wheat (*Triticum aestivum* L.). *Ecological Modelling,* 183 (2/3), 183-210.

Niinemets, U. and Tenhunen, J.D., 1997. A model separating leaf structural and physiological effects on carbon gain along light gradients for the shade-tolerant species *Acer saccharum*. *Plant, Cell and Environment,* 20 (7), 845-866.

Nikolov, N.T., Massman, W.J. and Schoettle, A.W., 1995. Coupling biochemical and biophysical processes at the leaf level: an equilibrium photosynthesis model for leaves of C 3 plants. *Ecological Modelling,* 80 (2), 205-235.

Von Caemmerer, S., 2000. *Biochemical models of leaf photosynthesis*. CSIRO Publishing, Collingwood.

Yin, X. and Van Laar, H.H., 2005. *Crop systems dynamics: an ecophysiological simulation model for genotype-by-environment interactions*. Wageningen Academic, Wageningen.